Structure of the Copper Cluster in Canine Hepatic Metallothionein Using X-ray Absorption Spectroscopy†

Jonathan H. Freedman,*,‡ L. Powers,§ and J. Peisach‡

Departments of Molecular Pharmacology and Molecular Biology, Albert Einstein College of Medicine, Bronx, New York 10461, and AT&T Bell Laboratories, Murray Hill, New Jersey 07974

Received June 18, 1985; Revised Manuscript Received December 31, 1985

ABSTRACT: The metal binding site in the lysosomal copper metallothionein from canine liver (LyCuLP) was examined with X-ray edge and extended X-ray absorption fine structure (EXAFS) spectroscopies. The *k*-absorption edge spectrum of LyCuLP was consistent with the coordination of univalent copper. The Fourier transform of the EXAFS data showed four resolved shells of backscattering atoms. Comparisons between the phase and amplitude functions derived from the isolated shells to those of Cu···Cu, Cu–S, and Cu–N model compounds showed that each copper was coordinated by four sulfur atoms at a distance of 2.27 ± 0.02 Å. Analysis of the outer shell data indicated backscattering copper atoms at 2.74 ± 0.05, 3.32 ± 0.05, and 3.88 ± 0.05 Å. Interatomic distances determined from the EXAFS data were compared to the distances observed by X-ray crystallographic analysis of adamantane-like clusters containing four and five copper atoms and a cubic cluster containing four copper atoms, structurally similar to the 4Fe-4S clusters in some ferredoxins. The results of these comparisons suggest that the copper complexed in LyCuLP is arranged in an adamantane-like cluster. The structure derived for this protein may be conserved in other copper metallothioneins.

In 1957, Margoshes and Vallee isolated a protein from equine renal cortex that was later named "metallothionein" (Margoshes & Vallee, 1957). Since that time, this protein has been isolated from other mammals, fish, invertebrates, and fungi (Kojima & Kägi, 1978, Nordberg & Kojima, 1979). Metallothioneins are low molecular weight, inducible proteins that bind a variety of metals including mercury, gold, lead, zinc, and copper (Winge et al., 1975, 1981). The function of the metallothioneins is not completely understood, although they are believed to be involved in the detoxification of heavy metals (Kojima & Kägi, 1978), the donation of metals to other metalloproteins during their synthesis (Lerch, 1980), and the maintenance of homeostatic levels of copper and zinc in tissue (Evans, 1973; Bloomer & Lee, 1978). Several pathological conditions are associated with the accumulation of copper, together with alterations in metallothionein levels. These include Wilson's disease (Evans et al., 1973; Scheinberg & Sternlieb, 1976), Menkes' disease (Menkes et al., 1962; Riordan & Jolicoeur-Paquet, 1982), and inherited copper toxicosis, an abnormality in Bedlington terriers similar to Wilson's disease (Twedt et al., 1979; Johnson et al., 1981).

The metal binding capacity of metallothionein, 4–11 mol of metal/mol of protein (Winge et al., 1981), is related to its high sulfhydryl content. Approximately 30% of the amino acid residues in the mammalian protein are cysteine (Lerch, 1981). There are no disulfide bridges or free sulfhydryl groups, and it is therefore believed that all of the cysteinyl sulfurs are directly involved in metal complexation (Kägi et al., 1974). Each metal ion is thought to be bound to four thiolates, with some of the sulfurs forming bridges between adjacent metal atoms (Otvos & Armitage, 1979). Cadmium-113 nuclear magnetic resonance studies with crab and rabbit metallothioneins have confirmed this arrangement and have shown that three or four metal atoms are organized into individual clusters (Otvos & Armitage, 1980; Otvos et al., 1982; Boulanger et al., 1983) for which two structures are proposed. The first is a cubic arrangement similar to that of the 4Fe-4S cluster of bacterial ferredoxins (Bordas et al., 1982), with each sulfur arising from a cysteinyl thiol. The second is a broken adamantane-like structure made of five- and six-membered rings composed exclusively of metal and thiol sulfurs (Vasak & Kägi, 1983).

Extended X-ray absorption fine structure (EXAFS)[1] spectroscopy has been previously used to examine the structures of sheep liver zinc metallothionein (Garner et al., 1982) and yeast metallothionein containing four copper atoms/mol (Bordas et al., 1982). Studies of both proteins showed that the metals were coordinated by four sulfur atoms. The zinc protein data were consistent with a single Zn–S bond distance of 2.29 Å. However, two different Cu–S distances were found for the yeast protein, 2.22 and 2.36 Å.

In order to define the structure of the copper binding site in a mammalian metallothionein that binds 7–9 atoms of copper, we studied the lysosomal copper liver protein (LyCuLP) isolated from Bedlington terriers (Johnson et al., 1981). Molecular weight, stoichiometry of metal binding, and comparisons of the amino acid composition and sequence (K.

† This investigation was supported in part by U.S. Public Health Service Grants AM-17702 (J.H.F.) and HL-13399 (J.P.). The synchrotron time was provided by the Stanford Synchrotron Radiation Laboratory, supported by National Science Foundation Grant DMR 77-27489, in cooperation with the Stanford Linear Accelerator Center and the U.S. Department of Energy. The data in this paper are from a thesis to be submitted by J.H.F. in partial fulfillment for the degree of Doctor of Philosophy in the Sue Golding Graduate Division of Medical Science, Albert Einstein College of Medicine, Yeshiva University.

* Address correspondence to this author at the Department of Molecular Pharmacology.

‡ Albert Einstein College of Medicine.

§ AT&T Bell Laboratories.

[1] Abbreviations: EXAFS, extended X-ray absorption fine structure; Cu–DTC, Cu(II)–diethyldithiocarbamate; Cu–TPP, Cu(II)–tetraphenylporphyrin; Cu(tmn), Cu(II)–*N*,*N*,*N*,*N*-tetramethylethylenediamine; LyCuLP, lysosomal copper metallothionein; eV, electronvolt; RS, thiol-containing compound; tu, thiourea; Ph-S, benzenethiol.

0006-2960/86/0425-2342$01.50/0

Lerch, personal communication) with those of known metallothioneins suggest that this protein is also a metallothionein. We conclude that four sulfur atoms are bound to each copper but at a single distance of 2.27 Å. Analysis of outer shell data show that copper atoms are at 2.74, 3.32, and 3.88 Å from the absorbing metal. In addition, analysis of the *k*-absorption edge data suggests univalent copper coordination.

Experimental Procedures

Sample Preparation. Lyophilized LyCuLP, provided by Drs. Richard Stockart and Irmin Sternleib of the Liver Research Unit, Albert Einstein College of Medicine, was prepared as previously described (Johnson et al., 1981). The protein was electrophoretically pure, showing a single band on 12% polyacrylamide gels. Atomic absorption spectroscopy showed that LyCuLP contained 7–8 mol of copper/mol of protein and was free of zinc. Samples for X-ray absorption measurements were prepared by dissolving 36 mg of protein in 0.3 mL of distilled, deionized water to yield a solution containing 12–15 mM protein and 80–120 mM copper. This was placed into a lucite sample holder (Powers et al., 1981) and frozen in liquid nitrogen.

Edge and EXAFS Measurements. X-ray absorption measurements were carried out at the Stanford Synchrotron Radiation Laboratory during dedicated operation of the SPEAR storage ring (40–80 mA at 3.04 GeV). Edge and EXAFS measurements were made exclusively at beam line I-5, which is an unfocused beam providing $\sim 1 \times 10^{10}$ photons/s with 1-eV resolution. The X-ray signal was measured by monitoring the fluorescence emitted by the sample with a seven fast-plastic scintillator array previously described (Powers et al., 1981). To decrease the background absorption due to elastic and Compton scattering, a nickel foil filter was placed between the sample and detector array (Stern & Heald, 1979). Due to the high metal concentration in the LyCuLP sample, only the center scintillator tube of the array was monitored. The incident intensity of the X-ray beam was determined with a nitrogen gas filled ionization chamber positioned between the sample and the defining slits (Powers, 1982).

The frozen protein sample was inserted into a cryostat of a design previously described (Powers et al., 1981), and the temperature was maintained at −140 °C to minimize the possibility of radiation damage (Peisach et al., 1982). Only six scans were necessary for the analysis because of the excellent signal to noise ratio. During the course of the experiment, no changes were observed in either the edge or EXAFS region of the spectra, demonstrating that radiation damage had not occurred at the metal binding site(s).

Data Analysis. Prior to analysis, the data were converted from a monochromator angle scale to an X-ray photon energy scale and standardized to the 4p edge peak of cupric chloride (8996 eV). A straight line background was subtracted from the edge and EXAFS data in order to remove the free atom contribution and any residual scattering effects from the absorption spectrum. The converted edge data were analyzed by comparing the energies of the electron transitions of the sample to those of copper complexes with known structures and oxidation states.

The EXAFS portion of the sample absorption spectrum was isolated from the background and/or isolated atom contributions by a cubic spline fit of the data, which was then multiplied by the cube of the photoelectron wave vector, k, to remove the $1/k^3$ dependence of the EXAFS (Eisenberger & Lengeler, 1980; Powers, 1982) and finally Fourier transformed. The contributions of each resolved shell, which corresponds to an absorber–scatterer distance, were back-transformed with a Fourier filter and resolved into their phase and amplitude functions (Lee et al., 1981). These functions for LyCuLP were compared to those for a copper–nitrogen model, Cu(II)–tetraphenylporphyrin (Cu–TPP), which has an average Cu–N distance[2] of 1.984 Å (Fleischer et al., 1964), and a copper–sulfur model, cupric diethyldithiocarbamate (Cu–DTC) with an average Cu–S distance of 2.316 Å (O'Connor & Maslen, 1966), by using the two atom-type fitting programs previously described (Brown et al., 1980). To determine Cu···Cu distances[2] in the higher shell data, copper metal and Cu(II)–*N*,*N*,*N*,*N*-tetramethylethylenediamine [Cu(tmn)], which have absorber–scatterer distances of 2.550 (Wasson et al., 1968) and 3.000 Å (Mitchell et al., 1970), respectively, were used as models. The EXAFS of the models were adjusted to exactly the same lengths, in k space, as the EXAFS of LyCuLP. Failure to make this correction resulted in inaccurate fittings and unreliable values for N_i and r_i.

Table I: Fit Parameters for Comparisons of Models[a]

model	sample	r_i (Å)	N_i	$\Delta\sigma_i^2$ ($\times 10^3$)	ΔE_0 (eV)	χ^2
Cu(tmn)	*Cu–Cu*	*3.00*	*1.00*	*−0.011*	*0.24*	*0.031*
	Cu–N	3.08	1.30	6.32	−4.06	3.02
	Cu–S	2.36	0.34	47.4	−6.55	21.0
Cu–TPP	Cu–Cu	1.93	2.19	−4.24	1.70	19.2
	Cu–N	*1.99*	*4.00*	*0.001*	*0.001*	*3.0×10^{-5}*
	Cu–S	2.13	2.76	−3.23	6.97	15.5
Cu–DTC	Cu–Cu	2.32	2.84	−5.18	2.89	35.2
	Cu–N	2.19	2.17	3.79	9.21	22.3
	Cu–S	*2.32*	*4.00*	*0.009*	*0.0001*	*1.0×10^{-5}*

[a] Parameters were calculated by using the fitting procedure described under Experimental Procedures. The terms r_i, $\Delta\sigma_i^2$, and ΔE_0 are the absorber–scatterer distance, change in Debye–Waller factor, and change in the threshold energy, relative to the model complex, respectively. χ^2 is the sum of residuals squared, which represents the goodness of fit. Italics denote the fit of the models to themselves and indicate the best fits of the data. The Cu–S, Cu–N, and Cu···Cu complexes listed as "sample" in the table were Cu–DTC, Cu–TPP, and Cu–tmn, respectively.

To calculate metal–ligand distances, LyCuLP data were compared to those of model copper complexes by fitting four parameters for each model to the sample data with the nonlinear iterated least-squares analysis procedure described by Brown et al. (1980). The parameters are, $\Delta\sigma_i^2$, ΔE_0, N_i, and r_i, where i is the type of backscattering atom. The Debye–Waller factor or thermal and lattice distortion parameter $\Delta\sigma_i^2$, which is highly correlated to N_i (Lee et al., 1981), and the threshold energy ΔE_0 are expressed as differences between the values for the protein sample and those of the models. N_i is the number of backscattering atoms at an average absorber–scatterer distance, r_i. The quality or "goodness" of the fit is indicated by the sum of residuals squared χ^2, calculated during the fitting procedure.

To determine which set of solution parameters represents the best fit of the LyCuLP data, acceptable limits of the various parameters were assigned. Limits for χ^2 and ΔE_0 were calculated by fitting the Fourier-filtered data of the various models to one another (Table I). This analysis showed that the worst fit of the experimental data provided a χ^2 near 22 for first shell analysis. Although this analysis demonstrated a maximum change in threshold energy of 9.2 eV, previous studies of other copper models have shown the largest acceptable ΔE_0 to be 16 eV (Powers et al., 1979). Fits that gave distances between directly coordinated absorber–scatterer pairs

[2] A solid line (–) between atoms indicates a covalent bond, whereas dots (···) indicate nonbonded absorber–scatterer pairs.

Table II: Fit Parameters for First Shell Filtered Data[a]

soln	r_N (Å)	r_S (Å)	$\Delta\sigma_N^2$ ($\times 10^3$)	$\Delta\sigma_S^2$ ($\times 10^3$)	$\Delta E_{0,N}$ (eV)	$\Delta E_{0,S}$ (eV)	χ^2
ON4S		*2.27*		*-0.81*		*-0.65*	*1.53*
1N3S	2.06	2.29	2.26	2.45	-5.45	-1.26	5.51
2N2S	2.08	2.30	-6.30	3.81	-6.23	-1.40	7.42
3N1S	2.10	2.31	-1.38	6.49	-6.98	-1.61	11.1
4N0S	2.14		1.91		-9.37		29.4

[a] The fit parameters were determined with the number of nitrogen (N) and sulfur (S) atoms held constant during the analysis. The parameters shown in italics are the best fits of the data, by the criteria described under Experimental Procedures. The errors for r_i (±0.02 Å) and $\Delta\sigma_i^2$ (±1.5 × 10^{-3} Å^2) delimit the range in which χ^2 doubles during the fitting procedure and were calculated as previously described (Shulman et al., 1978).

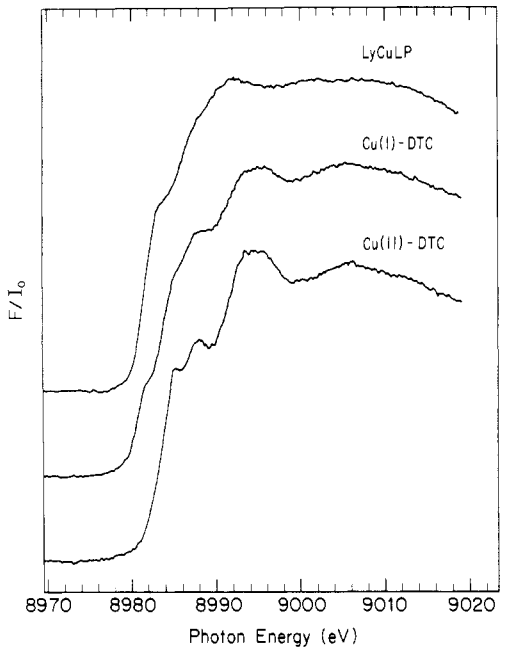

FIGURE 1: X-ray k-absorption edge of LyCuLP, Cu(I)–DTC, and Cu(II)–DTC. A linear background has been subtracted from the data, setting the absorption below the edge equal to zero. Data are expressed as the ratio of the fluorescence intensity (F) and the intensity of the incident radiation (I_0). Cuprous DTC, used for the analysis of absorption edge data, was prepared by reducing Cu(II)–DTC with an excess of dithionite under anaerobic conditions.

that are too long or too short, on the basis of X-ray crystallographic analyses, were rejected. Cu-N bond distances usually range between 1.95 and 2.20 Å and those for Cu–S between 2.18 and 2.40 Å. Values of $\Delta\sigma_i^2$ between -6.0×10^{-3} and 6.0×10^{-3} were considered acceptable since $\Delta\sigma$ for liquids is near 0.1 Å (Peisach et al., 1982).

Results

X-ray Absorption Edges. Peaks and shoulders in the k-absorption edge reflect transitions of 1s electrons into empty higher valence orbitals (Shulman et al., 1976). The edge spectra for LyCuLP, Cu(I)–DTC, and Cu(II)–DTC are shown in Figure 1. That for LyCuLP shows three features at 8984, 8988, and 8993 eV, which are tentatively assigned to the 1s–4s-, 1s–4p-, and 1s–np- ($n \geq 4$) like transitions, respectively. The transition energies of LyCuLP are similar to those of Cu(II)–DTC and Cu(I)–DTC. However, the transition energies and intensities of the protein spectrum most resemble those of the Cu(I)–DTC and suggest coordination of univalent copper in LyCuLP.

The presence of a 1s–3d transition, near 8975 eV, is often taken as a confirmation of the divalent oxidation state for copper (Hu et al., 1977). This transition is not observed in the LyCuLP spectrum, again suggesting coordination of monovalent copper. However, the inability to observe this transition is not taken as unequivocal proof of a univalent

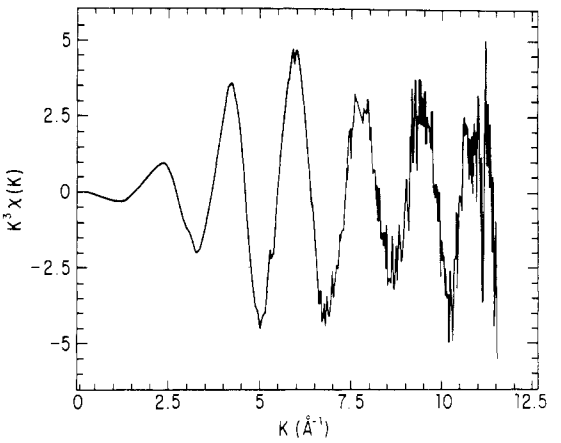

FIGURE 2: Background subtracted, k^3-multiplied, EXAFS modulation of LyCuLP. k is the wave vector calculated from the photon energy (Powers, 1982).

oxidation state, as it is absent for complexes in which divalent copper is covalently bonded to nitrogen or sulfur ligands, such as in butyraldehyde thiosemicarbazone and DTC (Powers et al., 1979).

The 1s–np transitions, near 8995 eV, of LyCuLP did not show any resolved structure. This may be due to slight inhomogeneities in the copper sites, and therefore, no assignment of the site symmetry could be made.

EXAFS. The background-subtracted, k^3-multiplied EXAFS is shown in Figure 2. The data for LyCuLP, as well as for Cu–DTC and Cu–TPP, were truncated to $k = 11.5$ Å^{-1} and these data Fourier-transformed (Figure 3). The most prominent peaks in the Fourier transforms, near 1.8, 2.5, 2.9, and 3.5 Å, represent backscattering contributions of the first and outer shell atoms. Data beyond 4 Å showed a dependence on the length of the EXAFS data set and therefore were not considered significant.

(*A*) *First Shell Analysis.* Solutions to the first shell data were determined, as described by Peisach et al. (1982), by fixing only the N_S and N_N parameters, allowing the other six parameters to vary. The best fit of the data was defined as one having the lowest χ^2 and parameters within the limits described above. The results in Table II show that the LyCuLP data are best described by a model in which the copper is coordinated by four sulfur atoms at a distance of 2.27 ± 0.02 Å. When nitrogen contributions are introduced into the model, χ^2 increases significantly. In addition, some of the parameters calculated for the nitrogen fits are greater than the acceptable limits.

It had been previously reported that two different Cu–S bond lengths, 2.36 and 2.22 Å, are found in yeast metallothionein containing four copper atoms per molecule (Bordas et al., 1982). To examine the possibility that unequal Cu–S bond lengths are present in LyCuLP, the data were fit to a four-sulfur model with different Cu–S bond distances (Table III). These results were calculated by setting the number of long and short sulfur bonds constant and allowing the other

Table III: Fit Parameters for First Shell Filtered Data Using Variable Cu–S Bond Lengths[a]

soln	r_L (Å)	r_S (Å)	$\Delta\sigma_L^2$ (×10³)	$\Delta\sigma_S^2$ (×10³)	$\Delta E_{0,L}$ (eV)	$\Delta E_{0,S}$ (eV)	χ^2
4L0S	*2.27*		*−0.82*		*−0.67*		*1.68*
3L1S	2.30	2.17	3.70	6.14	−1.33	2.34	4.82
2L2S	2.33	2.21	5.00	4.68	−1.78	0.95	5.02
1L3S	2.36	2.24	6.3	3.4	−2.89	0.15	5.38
0L4S		2.27		−0.82		−0.67	1.68

[a] Symbols are the same as defined in Table I. The fit parameters were determined with the number of long (L) and short (S) Cu–S bond lengths held constant during the analysis.

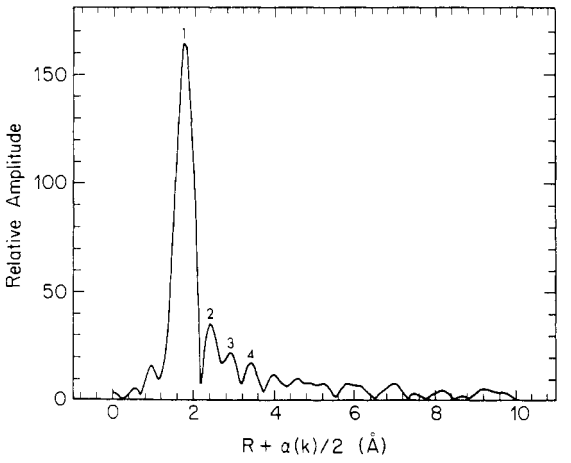

FIGURE 3: Magnitude of the Fourier transform of the k^3-multiplied data from Figure 2. R is the radial distance between the absorbing copper atom and the backscattering atoms and $\alpha(k)$ the energy-dependent absorber–scatterer phase shift. The peaks labeled 1–4 represent the backscattering contributions from the first, second, third, and fourth shell atoms, respectively.

parameters to vary. For all solutions, the introduction of unequal bond lengths caused a singnificant increase in χ^2 relative to the single-distance model. In addition, the $\Delta\sigma_i^2$ for the 3L1S and 1L3S models (see legend to Table III) were beyond acceptable limits. These results confirm that the best fit for LyCuLP is obtained with a single Cu–S distance of 2.27 Å.

The data were also fit to a model in which bond lengths of 2.36 and 2.22 Å, values reported for yeast metallothionein, were held constant and the other parameters allowed to vary. In this case χ^2, ΔE_0, and $\Delta\sigma_i^2$ were 6.7, −16.1 eV, and 6.7 × 10^{-3}, respectively. The values for ΔE_0 and $\Delta\sigma_i^2$ were not acceptable, and χ^2 was 4 times greater than for the single bond length model.

(B) Outer Shell Fit. The Fourier transform presented in Figure 3 shows a series of peaks, with intensities significantly greater than the noise level of the data, between $R + \alpha(k)/2$ = 2.5 and 3.5 Å. The peak near 2.5 Å may be a side lobe of the first shell peak and not represent an outer shell contribution. [Side lobes are mathematical artifacts produced by the Fourier transformation due to the finite length of the EXAFS data set (Powers, 1982; Woolery et al., 1984b).] If the 2.5-Å peak is a side lobe, a change in position would be observed as the length of the EXAFS data is shortened (Woolery et al., 1984a). As a shift was not detected, the 2.5-Å peak must contain a large contribution from an outer shell backscattering atom.

The resolved phase and amplitude functions from the isolated peaks were fit to Cu–N, Cu–S, and Cu···Cu models to determine the types of atoms in the outer shells and their distances. The procedures used to fit these data were similar to those for the first shell analysis except that the outer shells were fit to models containing either a single type of backscattering atom, N, S, or Cu, or pairs of atoms: Cu + S, Cu + N, or N + S. In the models containing pairs of backscattering atoms, the data were first fit to a single backscatterer. After a reasonable fit was obtained, the second atom was introduced into the model, and the sample data were refit to obtain the final solution. The constraints on ΔE_0 and $\Delta\sigma_i^2$ were similar to those used in the first shell analysis. However, no limit was imposed on absorber–scatterer distances, since the outer shell atoms are not directly bonded to the absorbing metal.

Table IV: Fit Parameters for Outer Shell Filtered Data Using Single Backscattering Atoms[a]

model	r_i (Å)	N_i	$\Delta\sigma_i^2$ (×10³)	$\Delta E_{0,i}$ (eV)	χ^2
			Second Shell		
Cu(tmn)	*2.74*	*0.35*	*1.62*	*−4.91*	*0.20*
Cu(metal)	2.79	0.23	3.54	−7.99	0.77
S	2.95	0.35	10.2	−2.36	0.30
N	2.82	0.45	8.11	−9.85	0.58
			Third Shell		
Cu(tmn)	3.32	0.30	1.71	9.21	0.22
Cu(metal)	3.35	0.23	2.66	6.95	0.24
S	3.29	0.32	9.83	10.1	0.14
N	3.39	0.47	7.12	4.34	0.10
			Fourth Shell		
Cu(tmn)	3.88	0.34	1.70	13.7	0.30
Cu(metal)	3.93	0.24	3.08	11.9	0.25
S	3.88	0.33	9.72	−5.94	0.04
N	3.97	0.51	7.26	9.11	0.13

[a] Symbols are the same as defined in Table I. Parameters displayed in italics for the second shell analysis are the best fit of the data for both single- and paired-atom fits (Table V), by the criteria described in the text. The Cu, N, and S models are Cu(metal) and Cu(tmn), Cu–TPP, and Cu–DTC, respectively. The errors in the distance measurements for the outer shells (±0.05 Å) were calculated as described in Table II.

Fit parameters calculated from the outer shell data with single- and paired-atom models are presented in Tables IV and V, respectively. The parameters shown in italics are the best fits of the data, on the basis of the criteria described below for each shell. These solutions were selected by first examining χ^2 and the magnitude of the disorder parameter, $\Delta\sigma_i^2$, for the single-atom fits and then comparing these results to the paired-atom fits. The paired-atom model was accepted as the best solution only when there was a significant improvement in the various parameters, as compared to single-atom fits.

The calculated N_i values were normally less than unity for fits of the outer shell data. When N_i was held constant at unity and the other parameters were allowed to vary, $\Delta\sigma_i^2$ decreased with little or no change in r_i and ΔE_0. There was always a 2–5-fold increase in χ^2, compared to the fits with variable N_i. The cause of this effect is not completely understood. However, Brown et al. (1980) made a similar observation when they examined the Cu···Cu distance in cupric acetate. Lee et al. (1981) addressed this problem in their discussion of the analysis of amplitude data, which is used to determine $\Delta\sigma_i^2$, N_i, and the types of atoms coordinated to the absorbing metal. They state that incorrect coordination numbers can be obtained

Table V: Fit Parameters for Outer Shell Data Using Pairs of Backscattering Atoms

atoms		atom 1 parameters				atom 2 parameters				
1	2	r_i (Å)	N_i	$\Delta\sigma_i^2$ (×10³)	$\Delta E_{0,i}$ (eV)	r_i (Å)	N_i	$\Delta\sigma_i^2$ (×10³)	$\Delta E_{0,i}$ (eV)	χ^2
					Second Shell					
Cu	N	2.72	0.34	1.8	−0.93	2.58	1.53	−27.5	−1.74	0.06
Cu	S	2.72	0.55	−0.70	−2.59	2.69	0.39	−3.25	0.94	0.12
N	S	2.79	0.16	13.5	−1.74	2.87	0.99	−7.37	0.25	0.12
					Third Shell					
Cu	*N*	*3.32*	*0.24*	*0.42*	*2.57*	*3.27*	*0.45*	*2.62*	*−6.79*	*0.06*
Cu	S	3.29	0.70	−2.54	12.5	3.29	1.20	−12.3	10.4	0.11
N	S	3.37	0.17	12.4	7.31	3.59	0.65	−8.13	3.75	0.03
					Second and Third Shells					
Cu	Cu	2.76	0.22	5.59	−10.9	3.31	1.10	−0.67	4.04	0.14
					Fourth Shell					
Cu	N	3.88	0.72	−2.88	12.9	3.67	0.92	−5.72	9.56	0.22
Cu	*S*	*3.88*	*0.24*	*0.57*	*3.87*	*3.90*	*0.60*	*6.03*	*−4.59*	*0.03*
N	S	3.84	0.60	6.96	4.44	3.87	0.66	10.1	−3.30	0.01

[a] Symbols are the same as defined in Table I. Parameters shown in italics for third and fourth shell analyses are best fits of the data for both single (Table IV) and paired atom fits, by the criteria described in the text. The Cu, N, and S backscattering are referenced to Cu(tmn), Cu–TPP, and Cu–DTC, respectively.

if the signal to noise ratio of the amplitude data is low, the length of the EXAFS data set is short, or the amount of disorder in the sample is high relative to the model system. All of these conditions may pertain to the LyCuLP sample and the outer shell data. In addition, it has been reported that amplitude transferability, i.e., using amplitude functions of models as standards for unknowns, is not as reliable when data are analyzed for models with chemical environments significantly different from those of the sample (Eisenberger & Lengeler, 1980; Stern et al., 1980). This effect is clearly demonstrated when model compounds were fit to one another (Table I). In these cases, correct values of N_i were observed only when a model was fit to itself. All other fits gave N_i values with errors ranging from 30 to 60%, in addition to significant increases in χ^2. Therefore, little significance is placed on calculated coordination numbers in the outer shells of LyCuLP.

Previous EXAFS studies of proteins containing multiple copper atoms have shown that, in addition to copper, peaks between 2 and 4 Å can result from backscattering C and N atoms in coordinated imidazole (Brown et al., 1980; Co et al., 1981a,b) or other low-Z atoms present in the protein, such as N, C, S, or O (Woolery et al., 1984b). As LyCuLP does not contain any histidyl residues, these peaks cannot be due to imidazole backscattering.

Since heavy atom scattering maximizes at higher k, it is strongly influenced when weighting factors are changed (Woolery et al., 1984b). Teo et al. (1977) determined that backscattering amplitudes maximized at higher values of k as the atomic number of the backscattering atom increased. To determine whether the outer shells contained copper and/or low-Z atoms, the effect on the Fourier transform of weighting the EXAFS data by k^2 vs. k^3 was examined. In cases where outer shells contain low-Z atoms, k^2 weighting causes an increase in the relative amplitude, compared to k^3 weighting. If the outer shell is a metal atom, k^2 weighting causes a decrease in the relative amplitude. A slight decrease or no change in peak amplitude indicates that the shell contains both low-Z and copper atoms (Woolery et al., 1984a). Weighting of the LyCuLP data by k^2 resulted in a slight decrease in the amplitude of peaks 2 and 3, and no change in peak 4, relative to the k^3 condition (Figure 3). These results suggest that the three outer shells contain copper and low-Z atoms. It has also been shown that the amplitude functions from the back-transformed data of hemocyanin and laccase, which contain multiple copper atoms, maximized at higher k for copper, compared to nitrogen or carbon atoms (Brown et al., 1980; Woolery et al., 1984a,b). The amplitude function of the first shell filtered data of LyCuLP, which is due exclusively to Cu–S interactions, maximized near 6 Å^{-1}. However, the functions for the outer shell data of peaks 2–4 maximized near 10 Å^{-1}, supporting the hypothesis that these shells contain backscattering contributions from copper.

Fits of the second shell data provide the lowest χ^2 when Cu–S and Cu···Cu models were used (Table IV). The disorder parameter calculated for the S fit is larger than the acceptable limits, indicating that this model is not an acceptable solution. In the fits using pairs of atoms (Table V), the Cu + N model has the lowest χ^2, but the $\Delta\sigma_i^2$ for the N contribution is −27.5, making this solution unacceptable. Thus, the best model of the second shell data has a copper atom 2.74 ± 0.05 Å away from the absorbing metal.

Analysis of the third shell data (Table IV) shows comparable χ^2 for all four models. The $\Delta\sigma_i^2$ values for the S and N fits are greater than acceptable limits. A slight improvement in the fit of third shell data for two-atom models (Table V) rather than single-atom models (Table IV) was obtained. The lowest χ^2's were observed, though, for the Cu + N and N + S models. The $\Delta\sigma_i^2$ for each atom in the N + S fit was greater than acceptable limits, indicating it is a poor fit of the data and is therefore ruled out. Fitting the data to the Cu + N model caused a significant improvement in χ^2 and $\Delta\sigma_i^2$, compared to Cu and N atoms fit independently. These results confirm that the third shell contains Cu at 3.27 ± 0.05 Å and suggests a second atom, possibly N, near 3.32 ± 0.05 Å.

Due to the small separation between the second and third shells, the backscattering contributions of the combined shells were isolated with a single Fourier filter. The backtransformed data were analyzed by the two-atom fitting procedure, as described above, with Cu + Cu, Cu + N, and N + N models. With this fitting procedure, only the contributions of a single backscattering atom per shell can be determined. The best fit of the data, obtained with the Cu + Cu model (Table V), shows Cu atoms at 2.76 ± 0.05 and 3.31 ± 0.05 Å. Fits in which N atom contributions were introduced showed 4-fold increases in χ^2 and $\Delta\sigma_i^2$ greater than 3×10^{-2}. The N atom contribution in the third shell, observed above, was not seen because of the high Z of copper, which dominates the shell

Table VI: Comparisons of Distances Determined from EXAFS Data with Distances Determined from X-ray Crystallography of Cu–RS Models[a]

distance (Å)	absorber–scatterer disposition	models
2.27	Cu*–*S*	$Cu_1(tu)_4$, $Cu(tu)_9$, $Cu_5(Ph\text{-}S)_7$
2.74	Cu*–S–*Cu*	Cu_4(cube), $Cu_5(Ph\text{-}S)_7$
3.27	Cu*–S–*Cu*	$Cu_4(tu)_9$, $Cu_5(Ph\text{-}S)_7$
3.88	Cu*–S–*Cu*	$Cu_4(tu)_9$, $Cu_5(Ph\text{-}S)_7$

[a] Distance measurements calculated from the EXAFS data were compared to $Cu(tu)_4$, a single-copper model, $Cu_4(tu)_9$, a four-copper adamantane-like cluster, $Cu_5(Ph\text{-}S)_7$, a five-copper adamantane-like cluster, and the hypothetical four-copper cubic cluster described in the text [Cu_4(cube)]. From these comparisons, locations of absorber–scatterer pairs in LyCuLP are proposed. The absorbing copper is labeled with an asterisk (*) and the backscattering atom is shown in italics.

(Woolery, 1984b). These results, those from the fit of the individually resolved shells, and the effect of k^2 vs. k^3 weighting on the Fourier transform strongly suggest the presence of Cu atoms at 2.74 ± 0.05 and 3.32 ± 0.05 Å from the absorbing metal atom.

The analysis of fourth shell data (Table IV) gave reasonable χ^2 values for the single-atom fits of Cu and N models. However, the $\Delta\sigma_i^2$ for the N model was beyond the acceptable limit. The small χ^2 observed for the S model suggests that this atom may be in the fourth shell, even though the disorder parameter is large. Fitting of the LyCuLP data to paired-atom models results in the lowest χ^2's for the Cu + S and the N + S models (Table V). The disorder parameters in the N + S fit were greater than acceptable limits and indicate that this is not a good model for the data. The χ^2 for the Cu + S fit is lower than that observed for the single-atom fits of either Cu or S. In addition, the $\Delta\sigma_i^2$ for the S contribution is now within acceptable limits. This suggests that the fourth shell contains Cu at 3.8–4.0 Å together with a second type of atom, probably S.

In order to tentatively assign a structure to the metal site(s) in LyCuLP, the interatomic distances determined from the EXAFS analysis were compared to X-ray crystallographic structures of Cu(I)–RS models including $Cu(tu)_4$ (Okaya & Knobler, 1964), $Cu_4(tu)_9$ (Griffith et al., 1976), $Cu_5(Ph\text{-}S)_7$ (Dance, 1976b, 1978), and Cu_5(*tert*-butylthiolate)$_7$ (Dance, 1976a). In addition, the EXAFS results were compared to cuprous halide models, which form Cu_4 cubic structures (Churchill & Kalra, 1974a–c), and to a 4Fe-4S ferredoxin (Carter, 1977). Models showing interatomic distances similar to those observed in LyCuLP are summarized in Table VI. The results of these comparisons suggest that copper atoms located in the outer shells are coordinated to the absorbing metal atom by thiolate bridges and that the three nonequivalent Cu···Cu distances reflect differences in the Cu–S–Cu bond angle. With 2.27 Å as a Cu–S bond length (this paper), Cu–S–Cu angles of 74.3 ± 1.6, 94.0 ± 1.9, and 117.5 ± 2.5° were calculated for Cu···Cu distances of 2.74 ± 0.05, 3.32 ± 0.05, and 3.88 ± 0.05 Å, respectively. These values are within the limits of Cu–S–Cu bond angles for known Cu(I)–RS clusters.

Discussion

The analysis of the *k*-absorption edge spectrum suggests that the copper in LyCuLP is univalent. Previous studies of the oxidation state of copper in yeast (Weser et al., 1977), bovine liver (Hartmann & Weser, 1977), and *Neurospora* metallothioneins (Beltramini & Lerch, 1983) had also shown the metal to be univalent. The absence of cupric ion in these proteins is not unexpected, on the basis of the known copper–thiol chemistry. It has been shown that the addition of either Cu(II) or Cu(I) to an anaerobic solution of cysteine results in the formation of a Cu(I)–Cys complex (Kolthoff & Stricks, 1951; Stricks & Kolthoff, 1951). This observation has been reconfirmed by using a variety of sulfhydryl-containing ligands including glutathione, thiourea, and penicillamine (Vortisch et al., 1976; Karlin & Zubieta, 1979; Österberg et al., 1979). Stable complexes containing a Cu(II)–RS structure in a Cu(I)–Cu(II) mixed-valence complex have been prepared by anaerobically titrating a thiol with Cu(II) (Klotz et al., 1958; Schugar et al., 1976; Paul et al., 1976). However, Cu(II)–RS is only observed if the thiol:copper ratio is less than 2 (Klotz et al., 1958). At higher thiol concentrations only the Cu(I)–RS complex is obtained. Since LyCuLP and other metallothioneins have thiol:copper ratios between 2 and 3, with all of the sulfhydryls directly chelated to metal (Kojima & Kägi, 1978), it is unlikely that copper would be divalent.

Three higher shells are resolved in the Fourier transform of the EXAFS data from LyCuLP, and their analysis indicates that the absorbing metal is surrounded by three nonbonded copper atoms at distances of 2.74 ± 0.05, 3.32 ± 0.05, and 3.88 ± 0.05 Å. The presence of resolved higher shells suggests that the absorbing metal is coordinated in a highly organized structure, as has been observed for metallothioneins isolated from a variety of sources.

The EXAFS analysis shows the copper atoms to be directly coordinated to four sulfur atoms with a single bond length of 2.27 ± 0.02 Å. This Cu–S distance is very similar to the Zn–S bond length obtained from the EXAFS analysis of Zn–metallothionein (Garner et al., 1982). Copper–sulfur distances near 2.27 Å have also been determined for various Cu(I)–RS models from the X-ray crystallographic analysis.

It has been previously reported that the metals complexed in metallothionein are arranged in clusters. The structures of the clusters are not known. However, they are believed to be either cubic (Bordas et al., 1982) or adamantane-like (Boulanger et al., 1983). To determine which cluster is present in LyCuLP, interatomic distances between the outer shell copper atoms were compared to clusters of known structure. Our EXAFS data for LyCuLP do not support the cubic model and suggest a structure similar to either a Cu_4 or Cu_5 adamantane-like cluster.

Were a cubic cluster present in LyCuLP, Cu···Cu distances between 2.73 and 3.22 Å would be observed. (These hypothetical limits were determined by assuming Cu–S bond lengths of 2.27 Å and metal–ligand–metal bond angles of 74–90°, as found in cuprous halide and 4Fe-4S ferredoxin clusters.) Although a backscattering copper atom is observed at 2.74 Å, a cubic model does not account for copper atoms at 3.32 and 3.88 Å, as suggested by our analysis. Further, the formation of a cubic cluster is unlikely in view of known Cu(I)–RS chemistry. Cubic cluster have been observed in inorganic complexes composed of $[As_3CuI]_4$ and $[P_3CuI]_4$ (Churchill & Kalra, 1974c), $[P_3CuCl]_4$ (Churchill & Kalra, 1974a), $[P_3CuBr]_4$ (Churchill & Kalra, 1974b), and [CuI(pyridine)]$_4$ (Raston & White, 1976) but not with thiol-containing ligands. In the presence of thiols, Cu(I) forms linear polymers of $[CuRS]_n$ and $[Cu_2(RS)_3]_n$ (Vortisch et al., 1976), which, in the presence of excess ligand, form adamantane-like clusters (Griffith et al., 1976) or $Cu_4(RS)_9$ polymers (Varnka & Amma, 1966). In addition, the formation of a cubic cluster requires the sulfur atom of cysteine to be covalently bonded to four atoms, three Cu(I) and C_γ, a condition that is not a

reasonable chemical structure.

The outer shell Cu···Cu distances in LyCuLP, 3.32 and 3.88 Å, were comparable to those found in the $Cu_4(tu)_9$ cluster, a four-copper adamantane-like model (Table VI). The 2.74-Å distance in the protein is not found in this model and may be the result of a strained Cu–S–Cu bond angle (74°), not present in the $Cu_4(tu)_9$ crystalline model. The $Cu_5(Ph\text{-}S)_7$ cluster, which also has a distorted adamantane-like structure, does however contain a short, 2.74-Å, Cu···Cu distance. This suggests that the metal clusters in LyCuLP may contain five copper atoms, compared to what has been reported for the four-metal cluster in Cd–metallothionein (Otvos & Armitage, 1980; Otvos et al., 1982). In view of the recent observation that the metal clusters in metallothioneins are flexible and constantly changing conformation (Vasak et al., 1985), it is not possible at this time to distinguish between Cu_4 and Cu_5 structures.

Registry No. Cu(I)–DTC, 14039-26-0; Cu(II)–DTC, 13681-87-3; Cu(tmn), 18130-66-0; Cu–TPP, 14172-91-9; $Cu_1(tu)_4$, 36252-51-4; $Cu_4(tu)_9$, 60618-39-5; $Cu_5(Ph\text{-}S)_7$, 59465-28-0; Cu, 7440-50-8; S, 7704-34-9; N_2, 7727-37-9.

REFERENCES

Beltramini, M., & Lerch, K. (1983) *Biochemistry 22*, 2043–2048.

Bloomer, L. C., & Lee, G. R. (1978) in *Metals and the Liver* (Powell, L. W., Ed.) pp 179–213, Marcel Dekker, New York.

Bordas, J., Koch, M. H. J., Hartmann, H.-J., & Weser, U. (1982) *FEBS Lett. 140*, 19–21.

Boulanger, Y., Goodman, C. M., Forte, C. P., Fesik, S. W., & Armitage, I. M. (1983) *Proc. Natl. Acad. Sci. U.S.A. 80*, 1501–1505.

Brown, J. M., Powers, L., Kincaid, B. M., Larrabee, J. A., & Spiro, T. G. (1980) *J. Am. Chem. Soc. 102*, 4210–4216.

Carter, C. W. (1977) in *Iron-Sulfur Proteins* (Lovenberg, W., Ed.) Vol. 3, pp 157–204, Academic, New York.

Churchill, M. R., & Kalra, K. L. (1974a) *Inorg. Chem. 13*, 1065–1071.

Churchill, M. R., & Kalra, K. L. (1974b) *Inorg. Chem. 13*, 1427–1434.

Churchill, M. R., & Kalra, K. L. (1974c) *Inorg. Chem. 13*, 1899–1904.

Co, M. S., Hodgson, K. O., Eccles, T. K., & Lontie, R. (1981a) *J. Am. Chem. Soc. 103*, 984–986.

Co, M. S., Scott, R. A., & Hodgson, K. O. (1981b) *J. Am. Chem. Soc. 103*, 986–988.

Dance, I. G. (1976a) *J. Chem. Soc., Chem. Commun.*, 68–69.

Dance, I. G. (1976b) *J. Chem. Soc., Chem. Commun.*, 103–104.

Dance, I. G. (1978) *Aust. J. Chem. 31*, 2195–2126.

Eisenberger, P., & Lengeler, B. (1980) *Phys. Rev. B: Condens. Matter 22*, 3551–3562.

Evans, G. W. (1973) *Physiol. Rev. 53*, 535–570.

Evans, G. W., Dobois, R. S., & Hambidge, K. M. (1973) *Science (Washington, D.C.) 181*, 1175–1176.

Fleischer, E. B., Miller, C. K., & Webb, L. E. (1964) *J. Am. Chem. Soc. 86*, 2342–2347.

Garner, C. D., Hasain, S. S., Bremner, I., & Bordas, J. (1982) *J. Inorg. Biochem. 16*, 253–256.

Griffith, E. H., Hunt, G. W., & Amma, E. L. (1976) *J. Chem. Soc., Chem. Commun.*, 432–433.

Hartmann, H.-J., & Weser, U. (1977) *Biochim. Biophys. Acta 491*, 211–222.

Hu, V. W., Chan, S. I., & Brown, G. S. (1977) *Proc. Natl. Acad. Sci. U.S.A. 74*, 3821–3825.

Johnson, G. F., Morell, A. G., Stockert, R. J., & Sternleib, I. (1981) *Hepatology (Baltimore) 1*, 243–248.

Kägi, J. H. R., Himmelhoch, S. R., Whanger, P. D., Bethune, J. L., & Vallee, B. L. (1974) *J. Biol. Chem. 249*, 3537–3542.

Karlin, K. D., & Zubieta, J. (1979) *Inorg. Perspect. Biol. Med. 2*, 127–149.

Klotz, I. M., Czerlinski, G. H., & Fiess, H. A. (1958) *J. Am. Chem. Soc. 80*, 2920–2923.

Kojima, Y., & Kägi, J. H. R. (1978) *Trends Biochem. Sci. (Pers. Ed.) 3*, 90–93.

Kolthoff, I. M., & Stricks, W. (1951) *J. Am. Chem. Soc. 73*, 1728–1733.

Lee, P. A., Citrin, P. H., Eisenberger, P., & Kincaid, B. M. (1981) *Rev. Mod. Phys. 53*, 769–806.

Lerch, K. (1980) *Nature (London) 284*, 368–370.

Lerch, K. (1981) *Met. Ions Biol. Syst. 13*, 299–318.

Margoshes, M., & Vallee, B. L. (1957) *J. Am. Chem. Soc. 79*, 4813–4814.

Menkes, J. H., Alter, M., Steigleder, G. K., Weakley, D. R., & Sung, J. H. (1962) *Pediatrics 29*, 764–779.

Mitchell, T. P., Bernard, W. H., & Wasson, J. R. (1970) *Acta Crystallogr., Sect. B: Struct. Crystallogr. Cryst. Chem. B26*, 2096–2101.

Nordberg, M., & Kojima, Y. (1979) in *Metallothionein* (Kägi, J. H. R., & Nordberg, M., Eds.) pp 41–116, Birkhauser, Basel, Switzerland.

O'Connor, B. H., & Maslen, E. N. (1966) *Acta Crystallogr. 21*, 828–830.

Okaya, Y., & Knobler, C. B. (1964) *Acta Crystallogr. 17*, 928–930.

Österberg, R., Ligaarden, R., & Persson, D. (1979) *J. Inorg. Biochem. 10*, 341–355.

Otvos, J. D., & Armitage, I. M. (1979) *J. Am. Chem. Soc. 101*, 7734–7736.

Otvos, J. D., & Armitage, I. M. (1980) *Biochemistry 19*, 4031–4043.

Otvos, J. D., Olafson, R. W., & Armitage, I. M. (1982) *J. Biol. Chem. 257*, 2427–2431.

Paul, J. M., Birker, W. L., & Freeman, H. C. (1976) *J. Chem. Soc., Chem. Commun.*, 312–313.

Peisach, J., Powers, L., Blumberg, W. E., & Chance, B. (1982) *Biophys. J. 38*, 277–285.

Powers, L. (1982) *Biochim. Biophys. Acta 683*, 1–38.

Powers, L., Blumberg, W. E., Chance, B., Barlow, C. H., Leigh, J. S., Smith, J., Yonetani, T., Vik, S., & Peisach, J. (1979) *Biochim. Biophys. Acta 546*, 520–538.

Powers, L., Chance, B., Ching, Y., & Angiolillo, P. (1981) *Biophys. J. 34*, 465–498.

Raston, C. L., & White, A. H. (1976) *J. Chem. Soc., Dalton Trans.*, 2153–2156.

Riordan, J. R., & Jolicoeur-Paquet, L. (1982) *J. Biol. Chem. 257*, 4639–4645.

Scheinberg, I. H., & Sternleib, I. M. (1976) in *Trace Elements in Human Health and Disease* (Ananda, S. P., & Oberleas, D., Eds.) Vol. 1, pp 415–438, Academic, New York.

Schugar, H. J., Ou, C., Thich, J. A., Potenza, J. A., Lalancette, R. A., & Furey, W. (1976) *J. Am. Chem. Soc. 98*, 3047–3048.

Shulman, R. G., Yafet, Y., Eisenberger, P., & Blumberg, W. E. (1976) *Proc. Natl. Acad. Sci. U.S.A. 73*, 1384–1388.

Shulman, R. G., Eisenberger, P., Teo, B.-K., Kincaid, B. M., & Brown, G. S. (1978) *J. Mol. Biol. 124*, 305–321.

Stern, E. A., & Heald, S. M. (1979) *Rev. Sci. Instrum. 50*, 1579–1582.

Stern, E. A., Bunker, B. A., & Heald, S. M. (1980) *Phys. Rev. B: Condens Matter 21*, 5521–5539.
Stricks, W., & Kolthoff, I. M. (1951) *J. Am. Chem. Soc. 73*, 1723–1727.
Teo, B.-K., Lee, P. A., Simons, A. L., Eisenberger, P., & Kincaid, B. M. (1977) *J. Am. Chem. Soc. 99*, 3854–3856.
Twedt, D. C., Sternleib, I., & Gilbertson, S. R. (1979) *J. Am. Vet. Med. Assoc. 175*, 269–275.
Vasak, M., & Kägi, J. H. R. (1983) *Met Ion Biol. Syst. 15*, 213–273.
Vasak, M., Hawkes, G. E., Nicholson, J. K., & Sadler, P. J. (1985) *Biochemistry 24*, 740–747.
Vortisch, V., Kroneck, P., & Hemmerich, P. (1976) *J. Am. Chem. Soc. 98*, 2821–2826.
Vranka, R. G., & Amma, E. L. (1966) *J. Am. Chem. Soc. 88*, 4270–4271.
Wasson, J. R., Mitchell, T. P., & Bernard, W. H. (1968) *J. Inorg. Nucl. Chem. 30*, 2865–2866.
Weser, U., Hartmann, H.-J., Fretzdorff, A., & Strobel, G.-J. (1977) *Biochim. Biophys. Acta 493*, 465–477.
Winge, D. R., Premakumar, R., & Rajagopalan, K. V. (1975) *Arch. Biochem. Biophys. 170*, 242–252.
Winge, D. R., Geller, B. L., & Garvey, J. (1981) *Arch. Biochem. Biophys. 208*, 160–166.
Woolery, G. L., Powers, L., Peisach, J., & Spiro, T. G. (1984a) *Biochemistry 23*, 3428–3434.
Woolery, G. L., Powers, L., Winkler, M., Solomon, E. I., & Spiro, T. G. (1984b) *J. Am. Chem. Soc. 106*, 86–92.

Secondary Structure in Sea Anemone Polypeptides: A Proton Nuclear Magnetic Resonance Study†

Paul R. Gooley and Raymond S. Norton*
School of Biochemistry, University of New South Wales, Kensington 2033, Australia
Received October 10, 1985

ABSTRACT: Elements of secondary structure in the sea anemone polypeptides anthopleurin A and *Anemonia sulcata* toxin I have been defined with the following nuclear magnetic resonance (NMR) spectroscopic data: the pattern of nuclear Overhauser enhancement (NOE) connectivities observed in two-dimensional NMR spectra for protons along the polypeptide backbone, NOE's between protons on separate strands of the polypeptide backbone, peptide NH exchange rates, and NH–H^{α} spin–spin coupling constants. These two polypeptides contain a region of four short strands of antiparallel β-sheet but little or no α-helix. This region of β-sheet brings the aromatic rings of Trp-23 and -33 into close proximity to form the nucleus for a small hydrophobic region. A type II reverse turn involving residues 30–33 has also been defined. Our results are compared with previous predictions of the secondary structure of these polypeptides. The structures are also discussed in relation to that of a scorpion toxin that appears to bind to a similar site on the sodium channel of excitable tissue.

Sea anemones contain a series of polypeptides of molecular weight about 5000, which exert potent effects on excitable tissue. One of these polypeptides, anthopleurin A (AP-A),[1] isolated from the northern Pacific species *Anthopleura xanthogrammica* (Norton, 1981; Norton et al., 1978), exerts a selective, potent, positive inotropic effect on the mammalian heart, without affecting heart rate or blood pressure (Shibata et al., 1976; Blair et al., 1978). AP-A is more potent and has a higher therapeutic index in vivo (Scriabine et al., 1979) than the cardiac glycoside digoxin. Its activity appears to be due to a specific interaction with the sodium channel of cardiac tissue, which leads to a delay in inactivation of the channel and thus a lengthening of the action potential and a greater influx of sodium ions (Kodama et al., 1981).

Other members of this homologous series of polypeptides for which amino acid sequences have been determined include anthopleurin C (Norton, 1981; Norton et al., 1978) from the anemone *Anthopleura elegantissima* and toxins I (Wunderer & Eulitz, 1978), II (Wunderer et al., 1976), and V (Scheffler et al., 1982) from the Mediterranean species *Anemonia sulcata*. The most thoroughly investigated of these is *Anemonia sulcata* toxin II (ATX II), which acts on the mammalian heart (Ravens, 1976) and on various nerve preparations (Bergman et al., 1976; Romey et al., 1976) by the same mechanism as AP-A, that is, by delaying inactivation of the sodium channel. Indeed, a considerable effort has been devoted to characterizing the mechanisms of action of these polypeptides (Beress, 1982; Alsen, 1983). By contrast, very little detailed information is available on their structures in solution. AP-A has been investigated by laser Raman, circular dichroism, and fluorescence spectroscopy (Ishizaki et al., 1979), as well as by natural abundance ^{13}C NMR spectroscopy (Norton & Norton, 1979, 1980; Norton et al., 1982). ATX II has been the subject of laser Raman (Prescott et al., 1976) and ^{13}C NMR (Norton et al., 1980) spectroscopic studies. While some information about the overall strutures of these molecules, as well as the local environments of specific residues, has emerged from these investigations, a detailed picture of their structures in solution

† Financial support by the Australian Research Grants Scheme is gratefully acknowledged.
* Address correspondence to this author.

[1] Abbreviations: AP-A, anthopleurin A; ATX I, *Anemonia sulcata* toxin I; ATX II, *Anemonia sulcata* toxin II; DSS, sodium 4,4-dimethyl-4-silapentane-1-sulfonate; NOE, nuclear Overhauser enhancement; COSY, two-dimensional homonuclear correlated spectroscopy; NOESY, two-dimensional homonuclear dipolar exchange spectroscopy.

0006-2960/86/0425-2349$01.50/0